paper reference: 5N.206

NOTCH STRESS STRAIN DISTRIBUTION IN CHARPY V SPECIMEN / EXPERIMENTS AND MODELLING

B. Tanguy[1,2], R. Piques[1], L. Laiarinandrasana[1], A. Pineau[1]

[1] Ecole des Mines de Paris, Centre des Matériaux, UMR CNRS 7633
BP 87, 91003 Evry Cedex, France
[2] Corresponding author, e–mail: btanguy@mat.ensmp.fr

ABSTRACT

The knowledge of the stress–strain–temperature distribution ahead of the notch in impact Charpy V specimen is a key issue in modelling fracture toughness. In this study an attempt is made to compare the plastic strain distribution ahead of the notch root either experimentally or numerically . The experimental measurements rely on a calibration curve obtained by a recrystallization technique and the measurement of recrystallized grain size in the vicinity of a Charpy V–notch. The numerical calculations were made by F.E. method using 2D and 3D simulations, and isothermal/adiabatic conditions. An original constitutive equation taking into account the various domains of strain rate sensitivity is presented. A satisfactory agreement is observed between experimental and calculated notch strain distribution.

INTRODUCTION

Charpy V–notch impact test is certainly the most convenient and hence the most widely used method to determine fracture properties of steels. Usual informations derived from this test are the total energy absorbed to fracture and the variation of ductile–brittle transition temperature with various parameters including the effect of irradiation on pressurized water reactor (PWR) steel. However in spite of the numerous studies devoted to this test method the complexity of the loading conditions as well as contact conditions between the specimen and the supports still explains the lack of basic understanding of the measured values. The need for further studies to obtain fracture toughness data from tests on Charpy specimens is clear. In particular the application of the local approach of fracture to Charpy test requires a good knowledge of the stress–strain field ahead of the notch root. A number of studies have already been devoted to this topic (see e.g. [1, 2]). The aim of the present study is to contribute to a further understanding of the thermomechanical conditions prevailing in the notch tip process zone. This contribution includes both an experimental part on the measurement of notch plastic strains and a numerical part on the calculation of the notch stress–strain state using a constitutive equation developed for this purpose and F.E. simulations.
This study was performed on A508 (16MND5) steel (C=0.16, Mn=1.33, Ni=0.76, Mo=0.51) which

bainitic steel measured at room temperature are : σ_Y=480 MPa, UTS=615 MPa.

MEASUREMENT OF NOTCH ROOT PLASTIC STRAINS

In the present study a recrystallization technique similar to that previously used by Shoji [3] and Lautridou [4] was applied to measure plastic strain at the notch root of a Charpy specimen. This method is based on the direct relationship between recristallized grain size and plastic strain in a given material. Tensile tests were carried out at different temperatures under quasi–static conditions ($\dot{\varepsilon}$ $\sim$0.0005 s^{-1}). These tests were interrupted before fracture in order to measure grain size as a function of the local plastic strain determined in the neck of the tensile specimen. After deformation, the specimens were recristallized at 695°C for 4 hours. The mean grain size $\bar{d}$ was measured on longitudinal sections while the local plastic strain $\bar{\varepsilon_p}$ was measured as $\bar{\varepsilon_p} = 2\ln\frac{\Phi_0}{\Phi}$, where Φ and Φ_0 are the actual and initial diameter of the smooth specimen, respectively. The results shown in figure 1, obtained on 3 specimens, indicate that the mean grain size is a decreasing function of applied plastic strain. In addition a threshold $\bar{\varepsilon_p}$ $\sim$25% is noted below which no recrystallization is obtained at least under the conditions used in the present study. The results shown in figure 1 are used as a calibration curve to assess the plastic strain ahead of the notch tip of a Charpy specimen.

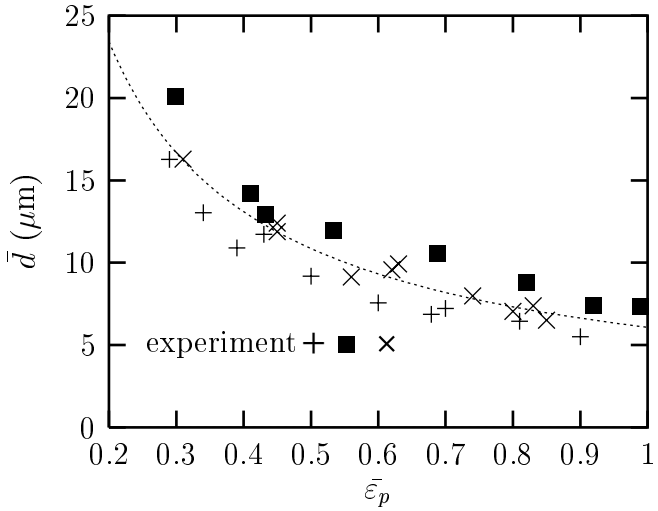

Figure 1: Recrystallized mean grain size, $\bar{d}$, as a function of equivalent plastic strain, $\bar{\varepsilon_p}$.

CONSTITUTIVE EQUATION

Several studies devoted to the simulation of Charpy V-notch test have outlined the important effect of strain rate and temperature on the failure modes in the ductile–brittle range see e.g. [5,6]. Due to steep gradient of plastic strain at the notch root, typical average strain rates of 3000 s^{-1} in quasi-static analysis (no inertial effects) were found in the failure process zone [1,5,7]. At these large strain rates, a significant increase of the flow properties is observed in mild steel [8]. This leads to an approximately linear variation of the flow stress with strain rate at constant temperature. At lower strain rates a single power law is usually observed. It appears therefore necessary to develop a constitutive law which is able to take into account these two strain rate regimes.

The constitutive equation presented in the present paper (called DIN) was developed to represent the temperature and strain rate sensitivity of the flow stress of A508 steel for a wide range of strain rate and temperature. The equations of the model are given in Table 1 where it is noticed that the strain rate sensitivity is described by a Double Inverse Norton (DIN) type expression. In this expression, R(ε_p,T) represents the strain hardening law under quasi–static conditions. This hardening is described by two isotropic components as shown in Table 2, where R_0(T) is the quasi–static yield stress at various

DIN Model	Equations from litterature
$\frac{1}{\dot{\varepsilon}} = \frac{1}{\dot{\varepsilon}_1} + \frac{1}{\dot{\varepsilon}_2}$ $\dot{\varepsilon}_{1,2} = \left\langle \frac{\bar{\sigma} - R(\varepsilon_p, T)}{K_{1,2}} \right\rangle^{N_{1,2}}$	$\bar{\sigma} = g(\varepsilon_p, T) \left(\frac{\dot{\varepsilon}_p}{\dot{\varepsilon}_0} \right)^m$ m$\sim$0.01, $\dot{\varepsilon}_0 \sim 0.02$ [11]
	$\bar{\sigma} = \sigma_0(\varepsilon_p, T) \left(\frac{\dot{\varepsilon}_p}{D} + 1 \right)^{\frac{1}{p}}$ p$\sim$10, $D \sim 0.132 \times 10^{11}$ [12]

TABLE 2
Strain hardening law of DIN Model

Strain hardening law	$R(\varepsilon_p, T) = R_0(T) + Q_1(1 - e^{-b_1 \varepsilon_p}) + Q_2(1 - e^{-b_2 \varepsilon_p})$
Temperature sensitivity of yield stress	$R_0(T) = \sigma_a + be^{-c(T+273.15)}$

temperatures. The DIN law includes 4 parameters (N_1,K_1,Q_1,b_1) which are temperature dependent and 7 constants (N_2,K_2,Q_2,b_2,σ_a,b,c). It is worth noting that the linear viscous effect observed at high strain rates is described by N_2 coefficient ($N_2 \sim 1$). The 11 coefficients included in this law were experimentally determined. In addition to quasi–static tensile tests ([-150°C , 200°C]) performed on a servohydraulic machine ($\dot{\bar{\varepsilon}} \sim 0.0005 s^{-1}$), dynamic compressive tests ([-100°C ; 20°C]) were carried out on a split Hopkinson–bar equipment ($\dot{\bar{\varepsilon}} \sim 3000 s^{-1}$). The results corresponding to intermediate strain rate (0.4 and 17.6 s^{-1}) were taken from [9]. Further details are given elsewhere [10].

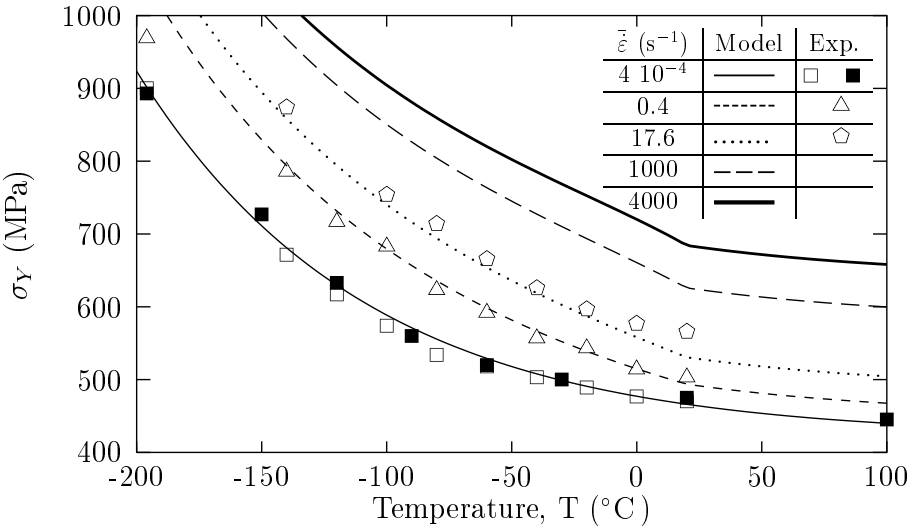

Figure 2: Yield stress versus temperature at different strain rates. Comparison with experimental data (Open symbols are taken from [9])

Figure 2 shows the variation of yield stress with temperature at different strain rates. Experimental data are included for comparison. It should be noted that above 20°C it is supposed that the strain rate sensitivity of the yield stress is the same whatever the temperature. This is only one approximation

DIN model and two other models taken from litterature is reported in figure 3a for two temperatures (-90 and 20°C). The model issued from [11] uses a linear relationship between the logarithms of $\dot{\bar{\varepsilon}}_p$ and $\bar{\sigma}$ (see Table 1). This model only represents the variation of the yield stress with strain rate at intermediate strain rates ($\dot{\bar{\varepsilon}} \leq 10^2 s^{-1}$). The model taken from [12,13] usually named Cowper–Symonds (CS) law assumes a non–linear evolution of Log$\bar{\sigma}$ versus Log$\dot{\bar{\varepsilon}}_p$ (see Table 1). The parameters of this model were determined from tests similar to those of the present study [12,13]. The Cowper–Symonds law describes more correctly the variation of the yield stress over a broad range of strain rate. However this law seems to be inappropriate to represent the strain rate sensitivity at very large strain rates ($\geq 10^3 s^{-1}$), as shown in figure 3a. The adequacy of the DIN model to describe both strain rate and temperature effects is shown in figure 3b where a comparison with experimental data is made.
The application of the above constitutive equation to the numerical simulation of Charpy V–Notch specimen and the comparison with experimental measurements of plastic strain ahead the notch root are presented below.

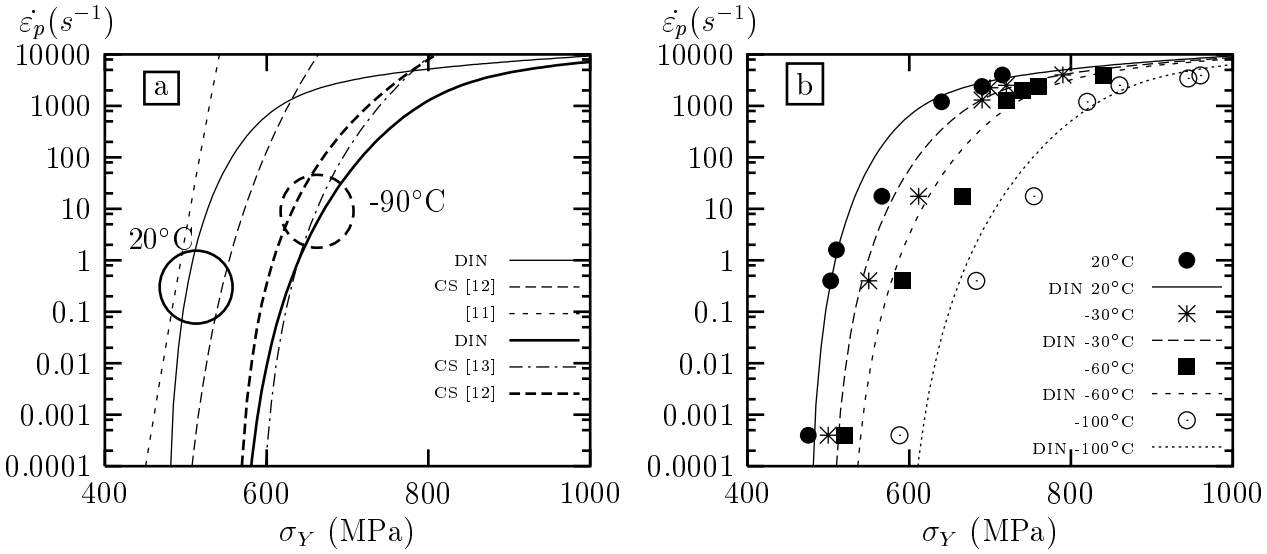

Figure 3: Variation of yield stress with strain rates at different temperatures. a) comparison between DIN model and other models in the litterature [11–13]. b) comparison between DIN model (curves) and experiments (symbols) at four temperatures, -100°C , -60°C , -30°C and 20°C

SIMULATION OF THE CHARPY TEST

In this part, various simulations of Charpy V–notch test were carried out using ZeBuLon code. Following the results obtained by Tahar [13], quasi-static modelling of Charpy test (i.e. neglecting inertial terms) was adopted. The shape of the striker and the anvil was taken from standard NF EN 10045–1. The mesh discretisation was based on triangular and square elements with quadratic displacement functions. Reduced integration was also used.

A combined 2D/3D mesh similar to that used by other authors [14] was adopted for the 3D analysis. Both isothermal and adiabatic modellings were made. For adiabatic conditions a Taylor–Quinney coefficient of 0.9 was used. All the simulations were performed with -80°C as initial temperature (lower part of the ductile–brittle transition range of this material). 2D simulations (plane stress and plane strain conditions) were also made. The anvils and the striker were modelled as rigid. Refined meshing was used to represent the contact areas between the specimen, the anvils and the striker. A detailed study about the influence of mesh size in the notch area was also made. Details are given elsewhere [15]. Here it is enough to say that the stress strain field at the notch root was found to be almost mesh size independent provided that the mesh dimension is below $\sim 100 \mu$m. The results given

the through–thickness mesh size was typically 1 mm.
In the present study which is devoted only to stress–strain state ahead of a Charpy V–notch, no attempts were made to simulate either cleavage or ductile fracture. This is the reason why the results shown in the following apply to moderate energy (∼40 Joules / hence moderate displacement). They apply therefore to the lower part of the ductile–brittle transition curve. Further studies are under progress to simulate fracture in particular to account for 3D effects which were shown to play a key role in other studies [16, 17].
Figure 4a shows the influence of the conditions used to simulate the load–displacement curve. This figure which refers to isothermal analysis clearly indicates that Charpy–V specimens must be modelled using 3D calculations. A detailed analysis of the experimental load–displacement curve and the 3D calculated one shows that above a displacement of the order of 2 mm, the experimental curve is located below the calculated one. This effect may be related either to the onset of ductile fracture or to the inadequacy of using isothermal conditions. This is illustrated in figure 4b where the stress–strain profiles at the notch are given. Extremely large strains of the order of 100% or even larger for plane stress simulations, are found close to the notch root. It is noted that the plane strain analysis applies to the mid–section of the specimen, as already shown by other authors [11–13]
The comparison between isothermal and adiabatic conditions is made in figure 5. A slight softening is observed on the overall load–displacement curve obtained with adiabatic analysis. This only produces a modification of absorbed energy of 4% for a 2.1 mm displacement. On the other hand, larger differences are observed on the stress profiles close to the notch as shown in figure 5b. In another study [15], it will be shown that this modification in stress profiles produces a significant effect on the calculation of the Weibull stress used in the Beremin model [18] to simulate cleavage fracture. The large strains shown in figure 5b generate a very significant temperature rise which can reach ∼300°C at the center of the specimen 5c. Further results not given here have shown that the calculated surface temperature is lower than the mid–section temperature. This means that a large attention must be paid to the significance of temperature surface measurements when a comparison between experiments and simulations is attempted.

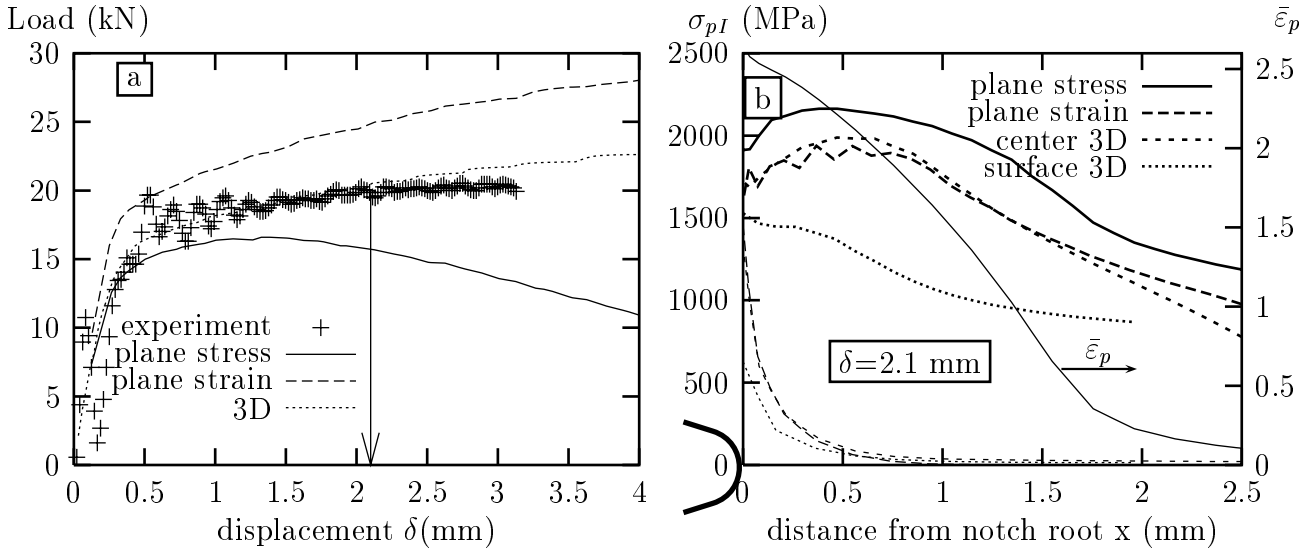

Figure 4: Influence of the analysis conditions on a) load–displacement curve and b) strain–stress state in the ligament. Isothermal (deformed mesh configuration).

The use of recrystallization technique to measure plastic strains at the notch root is illustrated in figure 6. Figure 6a shows the micrograph in the mid–sectionof a Charpy specimen corresponding to an interrupted test at -60°C (absorbed energy of ∼80 J). The specimen was submitted to the previous

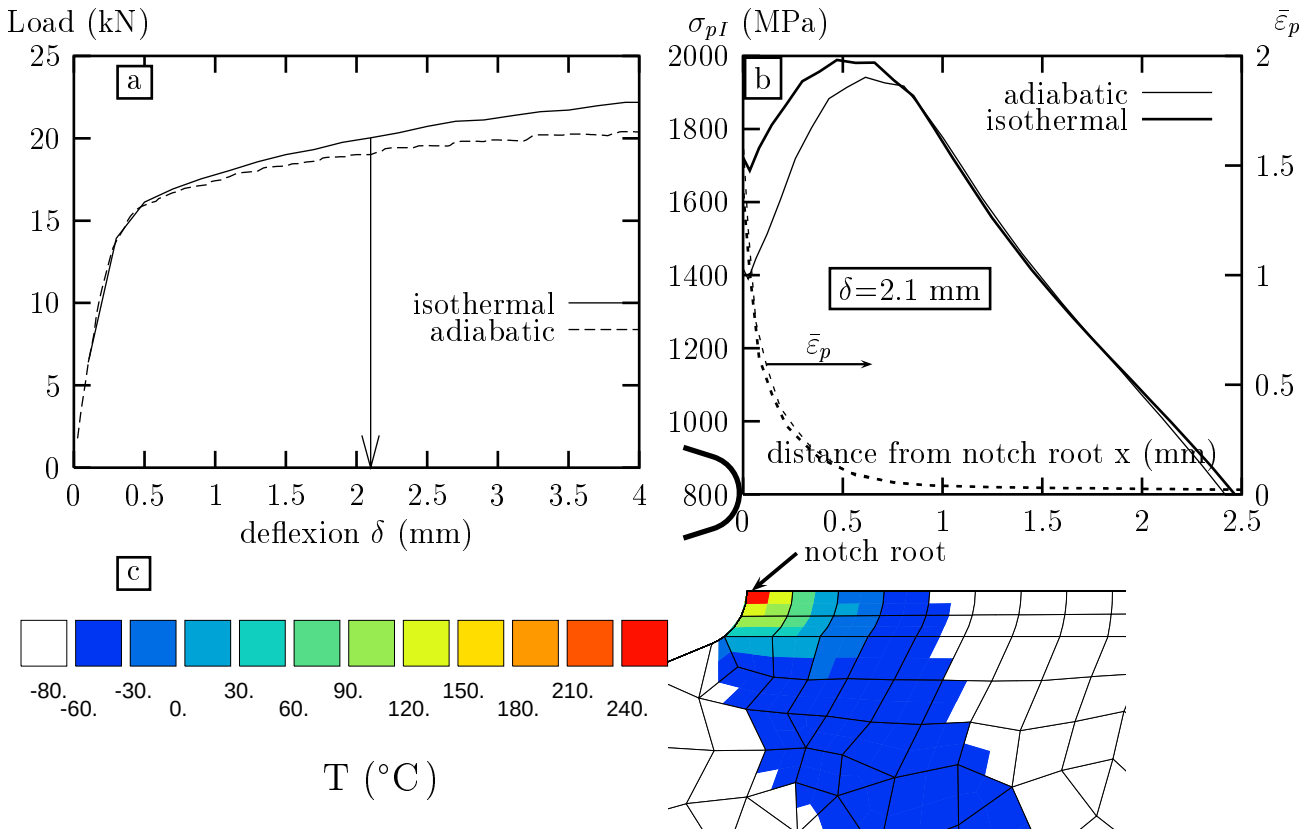

Figure 5: Comparison between isothermal and adiabatic 3D simulations. a) Load–displacement curve; b) stress–strain profile; c) temperature distribution

recrystallization heat–treatment after being tested. The micrograph of figure 6a clearly shows the presence of a small recrystallized grain area close to the notch root. The calibration curve given in figure 1 was used to assess the strains at the notch tip. Typical results are given in figure 6b and c corresponding to different test conditions. In both cases the scatter band is indicated. Figure 6b refers to a test carried out at -80°C under dynamic conditions (V_{impact}=5 ms^{-1}) while figure 6c corresponds to a test performed at -120°C at low rate (V_{impact}=0.5 mms^{-1}). In both cases the specimens broke by brittle cleavage fracture.

The comparison between calculated and measured strains is also made in figure 6b and c. In modelling the test performed at -80°C, a 3D simulation was made, taking into account adiabatic conditions because of the large impact rate. On the other hand the test carried out at -120°C was modelled using 2D isothermal conditions. The hypothesis about isothermal conditions is appropriate because of the slow impact rate. In addition it has been shown that at low temperature a 2D analysis was valid [12,13]. The results given in figure 6b and c show a satisfactory agreement between calculations and experiments. At -120°C a good agreement is observed. At -80°C the calculations seem slightly underestimate the measured strains very close to the notch tip. This might be due to a mesh size effect. However it should be noted that for large strains the slope of the calibration curve of figure 1 is such that a small variation in measured grain size leads to large variation in predicted plastic strains. Further studies using maps of plastic strains around the notch are being made.

CONCLUSIONS

1. The recrystallization technique developped in the present study is appropriate to assess plastic strain variations over the strain range between $\sim$ 30% and 80%.

2. The double inverse Norton law including two isotropic hardening components satisfactorily

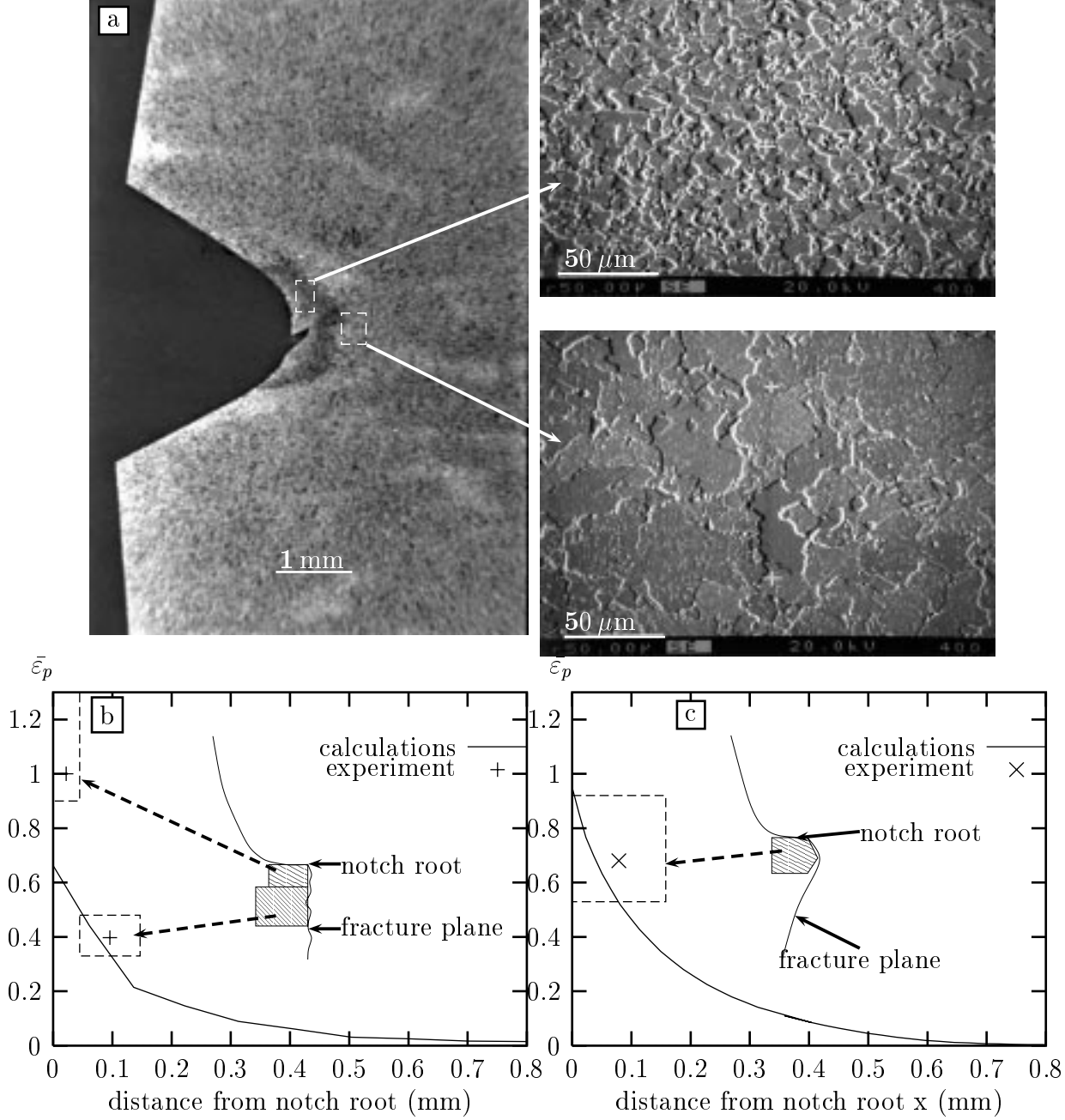

Figure 6: Mid–section strain distribution ahead of the notch in a Charpy specimen. a) Micrographs showing the reduction in grain size after recrystallization heat–treatment at the notch root; Comparison between experiment and F.E. calculations : b) dynamic Charpy test at -80°C (CVN=15 Joules) c) static test at -120°C (CVN=20.5 Joules)

describes the variation of the flow properties of A508 steel over a wide range of temperatures and strain rates. In particular this law accounts for the linear viscous effect observed at very large strain rates.

3. 3D adiabatic analysis of the Charpy test is necessary in particular to simulate large absorbed energies and large impact loading rates. Significant increases of temperature ahead of the notch root ($\sim$300°C) are calculated even for relatively moderate absorbed energy ($\sim$40 Joules).

4. A satisfactory agreement between calculated plastic strains around the notch root and the plactic strains measured with the recrystallization technique is observed.

Financial support from Direction de la sureté des installations nucléaires (DSIN) and Electricité de France (EDF) is acknowledged. Technical support from Y. Grandjean (EDF–Chinon), J. Clisson (CTA) and G. Brabant (EMP) is also greatly acknowledged. The authors would like to specially thank D^{r} J. Besson for his help in the numerical simulations.

References

1. Wilshaw, T.R. (1966) *J. Iron Steel Inst.*, **204**(9), 936.
2. Mohamed, S.A. and Tetekman, A.S. (1975) *Eng. Frac. Mechnics*, **7**, 631.
3. Shoji, T. (1976) *Metal Science*, 165.
4. Lautridou, J.C. (1980) PhD thesis, Ecole des Mines de Paris.
5. Tvergaard, V. and Needleman, A. (1986) *J. Mech. Phys. Solids*, **34**, 213.
6. Tvergaard, V. and Needleman, A. (1988) *Int. Jour. of Fracture*, **37**, 197.
7. Norris, D.M. (1979) *Eng. Fract. Mech.*, **11**, 261.
8. Campbell, J.D. and Ferguson, W.G. (1970) *Phil. Mag.*, **21**, 63.
9. Henry, M. and al. (1985) *Journal de mécanique théorique et appliquée*, **2**(6), 741.
10. Tanguy, B., Piques, R., Laiarinandrasana, L., and Pineau A. (2000) In *EUROMAT 2000, Advances in Mechanical Behaviour. Plasticity and Damage.* to be published.
11. Mathur, K.K., Needleman, A. and Tvergaard, V. (1993) *Modelling Simul. Mater. Sci. Eng.*, **1**, 467.
12. Rossol, A. (1998) PhD thesis, Ecole Centrale Paris.
13. Tahar, M. (1998) PhD thesis, Ecole des Mines de Paris.
14. Schmitt, W., Sun, D.Z. and Blauel, J.G. (1997) In *Recent advances in fracture*, pp 77–87. TMS.
15. Tanguy, B., Laiarinandrasana, L., Besson, J., Piques, R., and Pineau A. (2001) In *Charpy Centenary Conference CCC2001.* to be published.
16. Schmitt, W., Böhme,W. and Sun, D.Z. (1994) In *ECF10, Structural Integrity*, pp 159–170.
17. Mathur, K.K., Needleman, A. and Tvergaard, V. (1994) *Comput. Methods Appl. Mech. Engrg.*, **119**, 283.
18. Beremin, F.M. (1983) *Met. Trans.*, **14A**, 2277.